Progress In Electromagnetics Research B, Vol. 1, 237–252, 2008

PROBING THE FEED LINE PARAMETERS IN VIVALDI NOTCH ANTENNAS

J. H. Shafieha, J. Noorinia, and Ch. Ghobadi

Department of Electrical Engineering
Urmia University
Urmia, Iran

Abstract—Some new parameters in Vivaldi Notch antennas are debated over in this paper. They can be availed for the bandwidth application amelioration. The aforementioned limiting factors comprise two parameters for the radial stub dislocation, one parameter for the stub opening angle, and one parameter for the stub's offset angle. The aforementioned parameters are rectified by means of the optimization algorithm to accomplish a better frequency application. The results obtained in this article will eventually be collated with those of the other similar antennas. The best achieved bandwidth in this article is 17.1 GHz.

1. INTRODUCTION

Vivaldi Notch Antenna is a ultra wideband antenna of the TSA (Tapered Slot Antenna) cast which is also known as a patch slot antenna such as rectangular slot antenna [1], circular slot antenna [2], or Hilbert slot antennas [3]. Lewis propounded TSA antennas for the first time in 1974 [4]. TSA Antennas are abundantly utilized in mobile telecommunications and radars owing to their low-price and minuscule dimensions. P. J. Gibson proffered a new type of such antenna whose slot opened exponentially which was called Vivaldi antenna [5], that is why Vivaldi antennas are also called ETSA (Exponential Tapered Slot Antenna). Vivaldi Notch antennas can provide bandwidths up to several octaves. Bandwidth in this paper pertains to S_{11} which is typically $S_{11} < -10\,\mathrm{dB}$. S_{11} or SWR Parameters are among the prominent ones in antenna design.

Some other casts of TSA single antennas have been submitted whose best bandwidths is 1–18 GHz in Vivaldi antennas whose antenna is balanced antipodal [6, 7], 2.7–11 GHz in antipodal Vivaldi antenna

[8], and 1.2–9.9 GHz in Vivaldi without cavity with open extremities [9] but the above quantity Vivaldi antennas bearing multi arm feed line ranges from 2 to 12 GHz [10]. The dimensions of balanced antipodal Vivaldi Antenna is much large than the one proposed in this article. The bandwidth of other antennas is less than the one devised in this article.

Antenna's feed line and its relation to the bandwidth specifications are momentous and this fact is evident in some papers [4, 11]. Specimens of Vivaldi Notch Antenna along with the germane parameters [12] are illustrated in Figure 1.

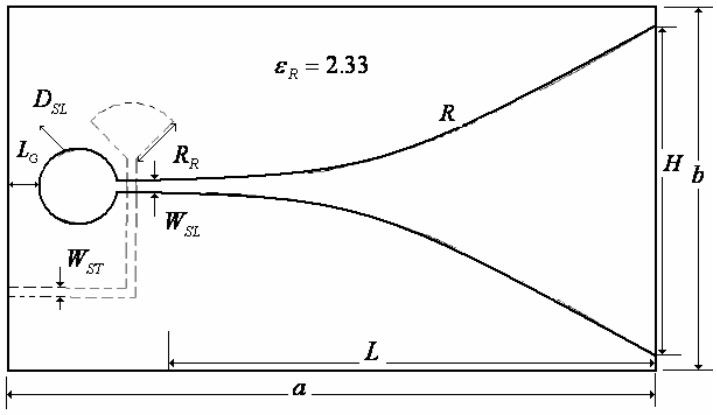

Figure 1. Vivaldi notch antenna.

$R_R = 1$ cm the radius of radial stripline stub

$W_{SL} = 0.5$ cm the antenna's stripline width

$W_{ST} = 0.5$ cm the microstrip feed line width

$L_G = 0.55$ cm the distance between the antenna's extremity and the cavity

$D_{SL} = 1.7$ cm the diameter of the slotline circular cavity

$R = 0.3\,\text{cm}^{-1}$ the opening rate of the slot in the slotline

$H = 8$ cm the antenna's aperture height

$b = 8$ cm the antenna's width

$a = 15$ cm the antenna's length

$L = 12.75$ cm the length of the open section of the slot

$t = 0.07874$ cm the thickness of the substrate

The antenna's aperture height discrepancy in single and array antennas have been alluded to in references [4, 13].

Some other limiting factors along with the aforementioned ones are presented in this article in order to survey their effects upon the antenna's bandwidth and the frequency application. Studies made over the above upshots are for the sake of ameliorating antenna's design and its frequency application. Longitudinal and latitudinal effects of dislocation of the feed line radial stub are probed in this paper and their role in the betterment of the frequency application will be delineated. The radial stub angle and the pertinent offset angle will be depicted afterwards to specify their effect upon frequency application. The above parameters will be opted for and manipulated to devise a better antenna.

The whole diagrams in this article have been simulated by means of HFSS Software and they have been illustrated by MATLAB Software.

2. THE RADIAL STUB DISPLACEMENT

The radial stub (hereinafter yclept stub) displacement can be defined in two ways: longitudinal and latitudinal dislocations, the aforementioned displacements have been delineated in Figure 2.

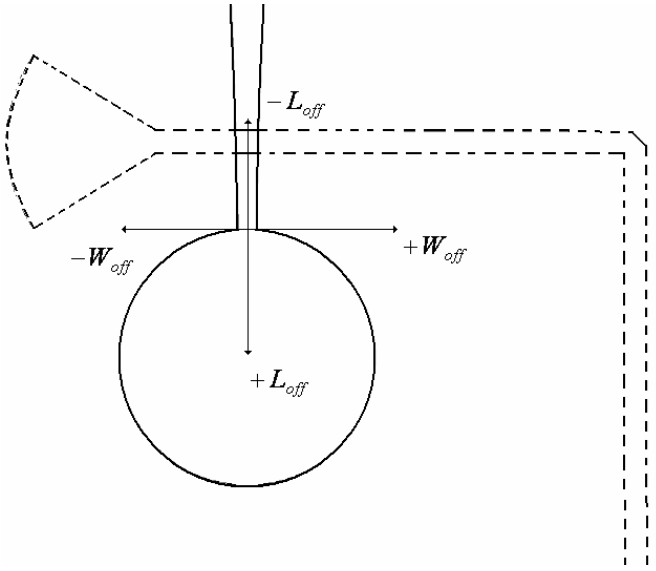

Figure 2. Dislocation of the radial stub.

If the feed line stub is displaced along the antenna's axis, its dislocation will be longitudinal displacement. The longitudinal stub displacement will be defined by L_{off}. The positive and negative quantities of L_{off} have been particularized in Figure 2. The zero location is designated as the intersection of the slotline and the slot cavity. If any motion towards the cavity occurs, L_{off} quantity will be positive otherwise negative in the counter direction. If stub moves along the antenna's width, its dislocation will be latitudinal displacement, which is stipulated by W_{off}. If the motion occurs on the dextral side of the department point (alias zero point) W_{off} will contain positive quantities, otherwise it will have negative values when motion occurs in the counter direction.

2.1. Radial Stub Longitudinal Dislocation

The high and low cutoff frequencies (for $S_{11} < -10\,\mathrm{dB}$) of Vivaldi Notch Antennas in term of L_{off} have been illustrated in Figure 3. The slotline width varies in accordance with the stub's longitudinal dislocation in the antenna's axis where it coincides with the feed microstrip line. The slotline impedance varies together with the slot's width alteration as follows [14]:

$$\begin{aligned} Z \;=\; & 60 + 3.69 \sin\left[\frac{(\varepsilon_r - 2.22)\pi}{2.36}\right] \\ & + 133.5 \ln(10\varepsilon_r)\sqrt{\frac{W_{SL}}{\lambda_0}} \\ & + 2.81[1 - 0.011\varepsilon_r(4.48 + \ln\varepsilon)\left(\frac{W_{SL}}{h}\right)\ln\left(\frac{100h}{\lambda_0}\right) \\ & + 131.1(1.028 - \ln\varepsilon_r)\sqrt{\frac{h}{\lambda_0}} \\ & + 12.48(1 + 0.18\ln\varepsilon_r)\frac{\left(\dfrac{W_{SL}}{h}\right)}{\sqrt{\varepsilon_r - 2.06 + 0.85\left(\dfrac{W_{SL}}{h}\right)^2}} \end{aligned} \tag{1}$$

$$2.22 < \varepsilon_r < 9.8$$

$$0.0015 \le \frac{W_{SL}}{\lambda_0} < 1.0$$

$$0.006 \le \frac{h}{\lambda_0} < 0.06$$

λ_0 is the line wavelength.

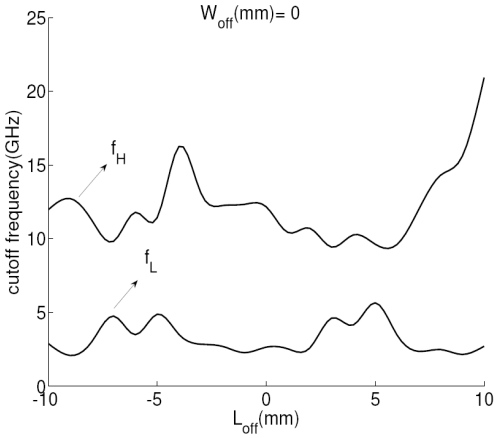

Figure 3. The cutoff frequencies alterations diagram in terms of the L_{off} and $W_{off} = 0\,\text{mm}$.

Hence if the slotline width alters, the slotline impedance will change too and it will affect the conveyance of the slotline to the microstrip line. It will eventually alter antenna's impedance. This matter affects impedance matching and S_{11} parameters.

The alterations of the microstrip line length are another determinant because line impedance changes as the line's length alters. The contributive effect of the two aforementioned factors changes the antenna's impedance and will eventually alter S_{11} too. The high cutoff frequency alterations (f_H for $S_{11} < -10\,\text{dB}$) exceed those of the low cutoff frequency (f_L for $S_{11} < -10\,\text{dB}$) because λ_H has a slight quantity in f_H diagram owing to the high frequency, ergo, any slight alternation in microstrip feed line length and the slotline width cause huge changes in impedance whereas λ_L has a higher value in f_L delineation due to the lower frequency. Thus it is less sensitive to microstrip feed line length alteration and the slotline width in impedance and eventually S_{11} value.

Thus the microstrip line length causes more sensitive in higher frequencies owing to the low value of λ. The same applies to the alteration of the slotline width. f_H and f_L optimum values can be achieved by the longitudinal displacement of the stub location, ergo; L_{off}'s value can be calculated in an optimum manner.

2.2. Radial Stub Latitudinal Dislocation

The cutoff frequencies alterations sketch has been outlined in Figure 4. Stub's location and its latitudinal displacement are the most significant

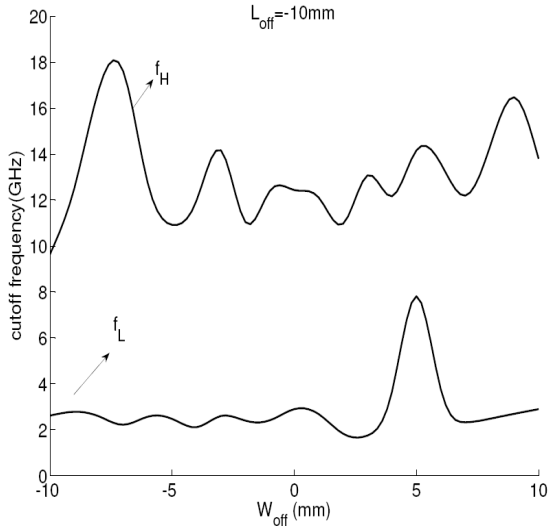

Figure 4. The cutoff frequencies alterations in terms of W_{off} and $L_{off} = 10\,\text{mm}$.

factors in the microstrip feed line length alteration and eventually the antenna's frequency application.

As it was mentioned in the previous section, this factor alters the terminal line impedance value in the diverse feed line wavelength of each frequency, furthermore, the above matter brings about S_{11} value alteration and the cutoff frequencies will change too. Observing f_L delineation, one notices that it entails mild alterations as compared with f_H diagram. The reason was explicated in the previous section. As λ_H value becomes lower than λ_L in the lower section cutoff frequency of f_L, length changes will have a more vehement effect upon them.

Optimum f_L and f_H value can be sought by the stub's latitudinal dislocation, thus, the best design can be achieved by optimization of the aforesaid parameter.

2.3. The Longitudinal and Latitudinal Dislocation of Stub and the Pertinent Relationship

Kindly pay attention to the diagrams in Figure 5. As depicted in the figure, W_{off} value alteration causes the variation of the corresponding f_L and f_H diagrams (in terms of L_{off}) with regard to diverse W_{off} values. Diverse W_{off} alterations cause variations in f_L and f_H diagrams (for $S_{11} < -10\,\text{dB}$) in terms of L_{off}, ergo, it is recommended to consider

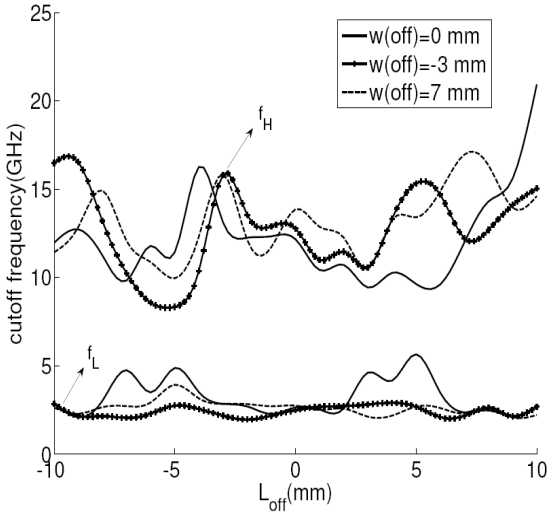

Figure 5. f_L and f_H diagrams for diverse W_{off}s in terms of L_{off}.

both parameters to peruse their effect upon frequency application. An optimum design necessitates the consideration of all the W_{off} and L_{off} modes.

Thus f_L and f_H values will alter in terms of L_{off} as W_{off} changes, ergo, both parameters are regarded simultaneously to make a flawless utilization of L_{off} and W_{off} parameters to ameliorate the antenna's frequency application. f_L and f_H 3-dimensional diagram in terms of L_{off} and W_{off} parameters have been illustrated in Figure 6.

Having made SQP† (Sequential Quadratic Programming) optimization algorithm amelioration in W_{off} and L_{off} alterations, the ensuing values will result: $W_{off} = 8\,\text{mm}$, $L_{off} = 2\,\text{mm}$. The bandwidth will rang from 1.7 to 16.4 GHz based upon the above values. SQP algorithm is a optimization algorithm similar to PSO‡ algorithm [15, 16] and genetic algorithm [17].

The diagram of L_{off} and W_{off} optimized values for f_L and f_H have been illustrated in figure 7 and compared with some other values. Optimization and frequency application betterment is evident as compared with other W_{off} and L_{off} values. The optimized low cutoff frequency $f_L = 1.7\,\text{GHz}$ and high cutoff frequency $f_H = 16.4\,\text{GHz}$ are sketched in Figure 7.

† Sequential Quadratic Programming
‡ Particle Swarm Optimization

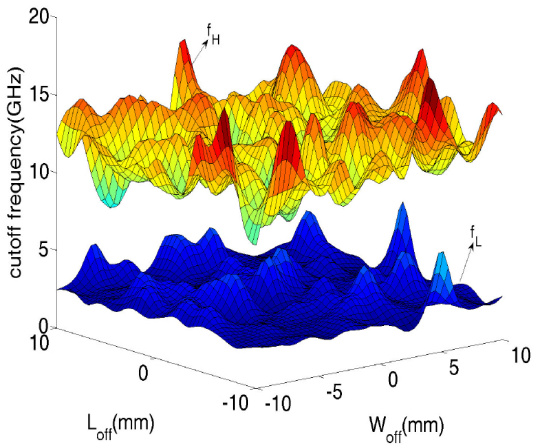

Figure 6. f_L and f_H 3-dimensional diagram in terms of L_{off} and W_{off}.

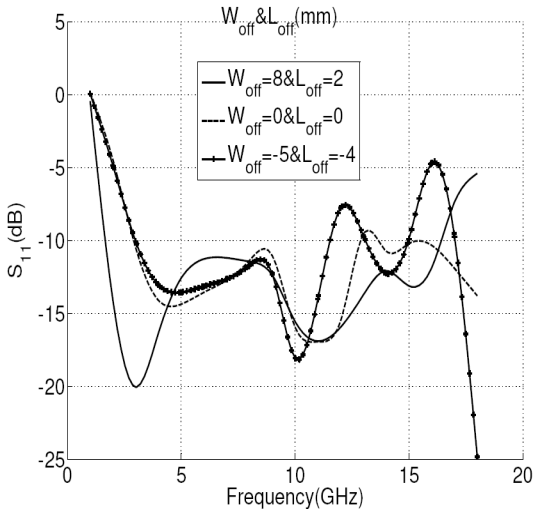

Figure 7. Collation of the bandwidth in the bettered ones and their comparison with some other W_{off} and L_{off} values.

3. STUB ANGLE AND STUB OFFSET ANGLE

The stub offset angle is defined by θ_{ST}. If OA' demi-line is a bisection of the stub angle ($A\hat{O}B$), and if OB' line is the horizontal line or the

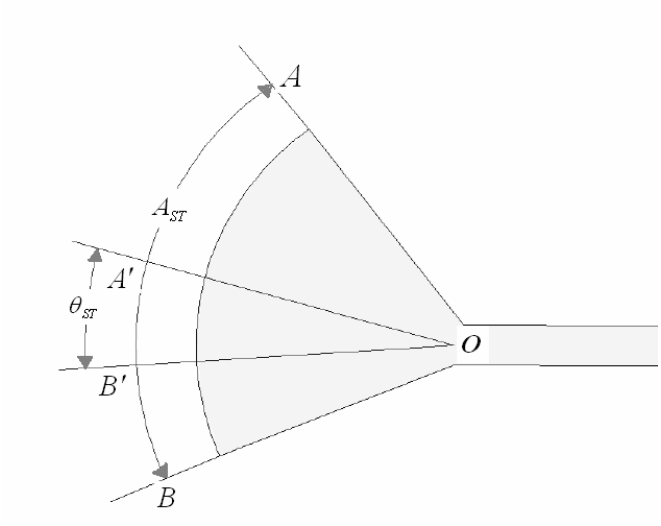

Figure 8. Stub offset angle and stub angle definition.

microstrip feed line axis, $A'\hat{O}B'$ angle will be defined as stub's offset angle. Parameters of the stub angle and stub offset angle have been illustrated in Figure 8. Stub angle is the same as opening angle of the radial stub which is specified by A_{ST} and is denoted in the Figure 8 as $A\hat{O}B$ Angle.

3.1. Stub Offset Angle

The impedance of the microstrip feed line antenna, and the cutoff frequencies are so sensitive towards the stub offset angle alteration. This matter is illustrated in Figure 9. f_L and f_H cutoff frequencies alteration diagram in terms of θ_{ST} changes is outlined in Figure 9.

As depicted, the high cutoff frequency alterations outstrip those of the low cutoff frequency. The cutoff frequencies alterations are not based upon a specific paradigm. The optimum θ_{ST} value can be achieved sheerly by optimization. f_H diagram is more sensitive to θ_{ST} alterations than f_L diagram due to slight value of λ in f_H frequencies. The only discrepancy between these two frequencies is their λ value.

3.2. Stub Angle

f_L and f_H alteration diagram is limned in Figure 10. $\theta_{ST} = 0^\circ$ in this diagram and f_L alterations are relatively mild whereas f_H alteration have more fluctuations owing to the reasons mentioned in the previous section nonetheless f_H frequency alterations outstrip those of f_L.

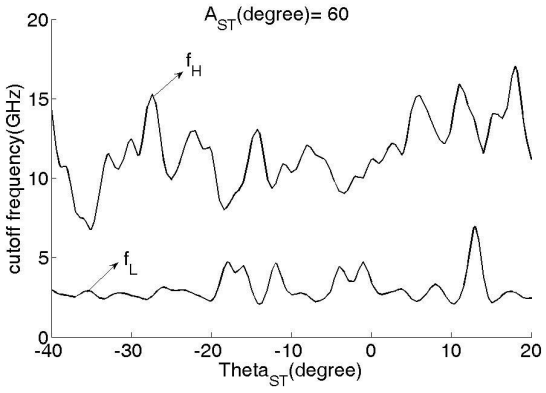

Figure 9. f_L and f_H alteration diagram in terms of θ_{ST} and $A_{ST} = 60°$.

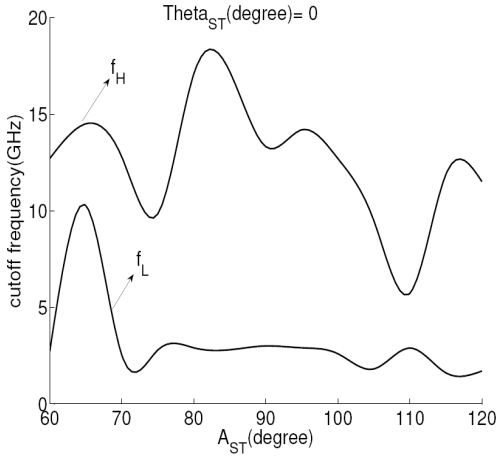

Figure 10. f_L and f_H alteration diagram in terms of $A_{ST}, \theta_{ST} = 0°$.

Since stub angle value alteration does not entail conjecturable increase or decrease the low and high cutoff frequency values, optimization methodology can be availed for parameter selection and antenna's design.

3.3. The Relation between Stub Offset Angle Alteration and Stub Angle

As illustrated in Figure 11, stub angle alteration cause changes in f_L and f_H cutoff frequencies in terms of offset angle variation, ergo, the

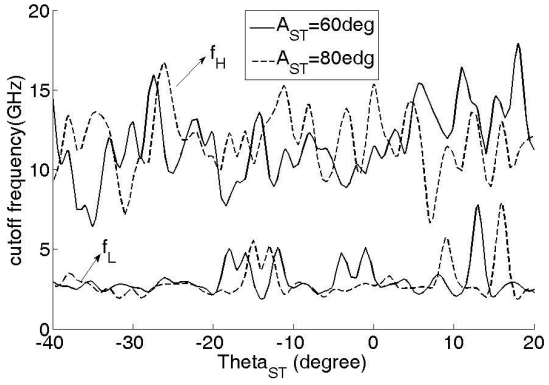

Figure 11. f_L and f_H diagrams for diverse A_{ST} in terms of θ_{ST}.

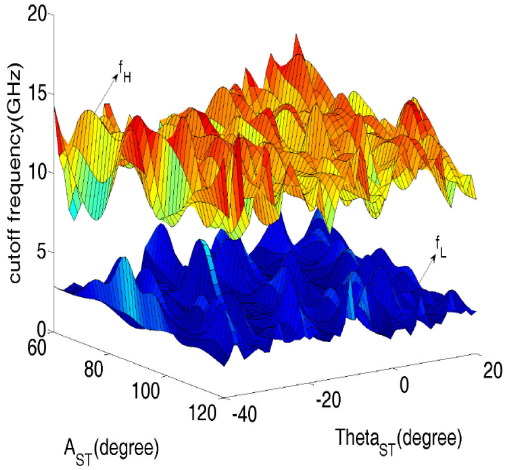

Figure 12. The 3-dimensional diagram of A_{ST} and θ_{ST} variations for the cutoff frequencies of f_L and f_H.

diagram will be modified.

The two parameters mentioned above are regarded simultaneously to accomplish an ideal delineation and to exploit all the potentials. This matter is limned in Figure 12. The 3-dimensional f_L and f_H diagram in terms of A_{ST} and θ_{ST} is illustrated in Figure 12. Both parameters can be generally taken into account in Figure 12 to actualize a better outline. Optimization algorithms can be availed to opt for the best A_{ST} and θ_{ST} values. SQP algorithm has been utilized

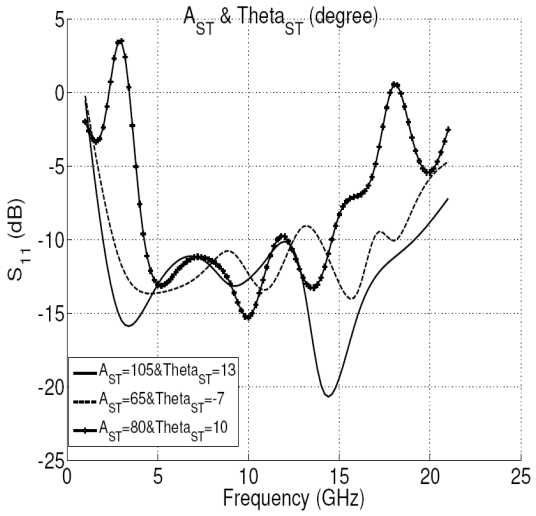

Figure 13. Collation of the bandwidth between the optimized parameters and some other A_{ST} and θ_{ST} values.

here too.

The aforementioned parameters can be figured out through this algorithm as follows $\theta_{ST} = 13°$, $A_{ST} = 105°$. The bandwidth will range from 2 to 19.1 GHz based upon the above values. The aforesaid parameters will be chosen only if f_L and f_H cutoff frequencies variation does not pass beyond a specific amount so that the working upshots and the frequency application won't differ a great deal in case any errors transpire in the manufacturing process.

As illustrated in Figures 9 and 10, some of the parameters have the optimum slightest f_L and the best f_H values to achieve the ideal bandwidth nonetheless the low and high cutoff frequency values of the points juxtaposed to them do differ a great deal owing to the reasons cited beforehand. Such points can't be appropriate for antenna delineation, ergo, the point observed in this article is the fact that the cutoff frequencies of the adjacent points of A_{ST} and θ_{ST} actualized due to optimization do vary slightly from the cutoff frequencies accomplished in optimum values, hence, the above matter has been mused over in the values worked out for A_{ST}, θ_{ST}, L_{off} and W_{off} values which have been computed through SQP optimization algorithm. Rectification of A_{ST} and θ_{ST} values can be easily apprehended based upon the Figure 13.

The discrepancy between the cutoff frequencies of the optimized values of A_{ST} and θ_{ST} and some other parameters are obviously

depicted in Figure 13. The nonpareil 17.1 GHz bandwidth has been actualized in the optimization mode.

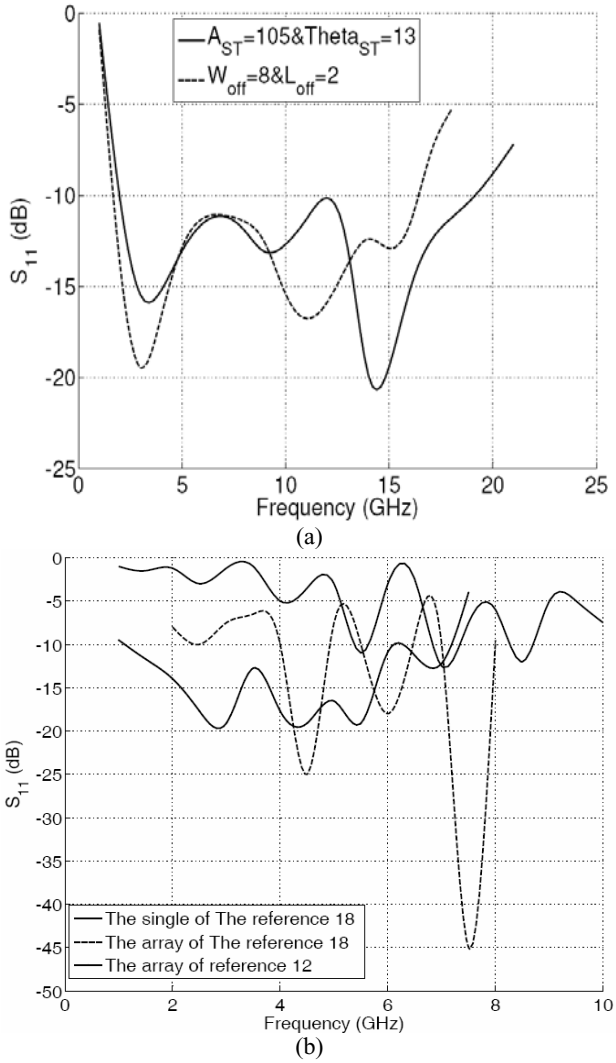

Figure 14. Differentiating this article's specimen with other similar ones (a) those outlined in the previous articles (b) antennas with optimized feed.

4. RESULT

The antennas outlined in this article are collated with those of the previous ones to get a better apprehension of the parameters alluded to in this article and to improve antenna's performance owing to the exploitation of the new parameters. Two antennas delineated in this article have been compared with similar single Vivaldi Notch Antennas depicted in [12, 18]. Antenna's rectified performance as compared with the previous tasks is quite evidence in Figure 14. The antennas devised in this article have a better performance the array-bearing ones which is quite conspicuous in the above figure, ergo, if new parameters are deliberated over and ameliorated by means of the prevalent mechanisms, a better henceforth antenna will be actualized.

5. CONCLUSION

Some new parameters have been proffered for Vivaldi Notch Antennas which are as follows: two parameters for radial stub dislocation, one parameter for stub opening angle, and one parameter for stub offset angle. The effect of the above parameters upon frequency application was checked based upon the S_{11} features as well as the cutoff frequency reaction in $S_{11} < -10\,\mathrm{dB}$. The optimum values were achieved for the aforementioned parameters by means of SQP algorithm and the ameliorated values were collated with other ones.

Since these parameters are interconnected (namely L_{off} with W_{off} and A_{ST} with θ_{ST}), they have been optimized concomitantly.

The upshots of the aforementioned optimization and the rectified parameters were manifest in microstrip feed line of Vivaldi Notch Antennas. The antennas worked out based upon the above parameters were collated with specimen of the previous delineations and their influence and optimization were noted. The best actualized result 17.1 GHz (2–19.1 GHz) pertained to $A_{ST} = 105^\circ$ and $\theta_{ST} = 13^\circ$.

ACKNOWLEDGMENT

Hereby the authors of this article express their gratitude to the Iran Telecommunication Research Center (ITRC) for bracing this research.

REFERENCES

1. Geran, F., G. Dadashzadeh, M. Faris, N. Hojjat, and A. Ahmadi, "Rectangular slot with a novel triangle ring microstrip feed for

UWB applications," *J. of Electromagn Waves and Appl.*, Vol. 21, No. 3, 387–396, 2007.

2. Sadat, S., M. Fardis, F. G. Kharakhili, and G. Dadashzadeh, "A compact microstrip square-ring slot antenna for UWB applications," *Progress In Electromagnetics Research*, PIER 67, 173–179, 2007.
3. Sayem, A. M. and M. Ali, "Characteristics of a microstrip-FED miniature printed Hilbert slot antenna," *Progress In Electromagnetics Research*, PIER 56, 1–18, 2006.
4. Lewis, L. R., M. Fassett, and J. Hunt, "A broadband stripline array element," *Dig. 1974 IEEE Antennas Propagat. Symp.*, 335–337, Atlanta, GA, 1974.
5. Gibson, P. J., "The Vivaldi aerial," *Proc. 9th European Microwave Conference*, 103–105, 1979.
6. Gazit, E., "Improved design of the Vivaldi antenna," *IEEE Proceedings*, Vol. 135, Pt. H, No. 2, April 1988.
7. Langley, J. D. S., P. S. Hall, and P. Newham, "Novel ultrawide-bandwidth Vivaldi antenna with low crosspolarisation," *Electronics Letters*, Vol. 29, No. 23, November 11, 1993.
8. Mehdipour, A., K. Mohammadpour-Aghdam, and R. Faraji-Dana, "Complete dispersion analysis of Vivaldi antenna for ultra wideband applications," *Progress In Electromagnetics Research*, PIER 77, 85–96, 2007.
9. Yin, X., Z. Su, W. Hong, and T. J. Cui, "An ultra wideband tapered slot antenna," Center for Computational Electromagnetics and State Key Laboratory of Millimeter Waves, Department of Radio Engineering, Southeast University, Nanjing 210096, 2005.
10. Yoon, I. J., H. Kim, H. K. Yoon, Y. J. Yoon, and Y.-H. Kim, "Ultra-wideband tapered slot antenna with band cutoff characteristic," *Electronics Letters*, Vol. 41, No. 11, May 26, 2005.
11. Joardar, S. and A. B. Bhattacharya, "Two new ultra wideband dual polarized antenna-feeds using planar log periodic antenna and innovative frequency independent reflector," *J. of Electromagn. Waves and Appl.*, Vol. 20, No. 11, 1465–1479, 2006.
12. Schaubert and Shin, "A parameter study of stripline-fed Vivaldi notch-antenna arrays," *IEEE Trans. on Antennas and Propagation*, Vol. 47, No. 5, 879–886, May 1999.
13. Yngvesson, et al., "The tapered slot antenna — A new integrated element for millimeter-wave applications," *IEEE Transactions on Microwave Theory and Techniques*, Vol. 37, No. 2, 365–374,

February 1989.

14. Gupta, K. C., R. Garg, and I. J. Bahl, *Microstrip Lines and Slotlines*, Artech House, Dedham, MA, 1979.
15. Cedn, T. B., Y. L. Dong, Y. C. Jiao, and F. S. Zhang, "Synthesis of circular antenna array using crossed particle swarm optimization," *J. of Electromagn. Waves and Appl.*, Vol. 20, No. 13, 1785–1795, 2006.
16. Lim, T. S., V. C. Koo, H. T. Ewe, and H. T. Chuah, "High-frequency phase error reduction in SAR using particle swarm of optimization algorithm," *J. of Electromagn. Waves and Appl.*, Vol. 21, No. 6, 795–810, 2007.
17. Mitlineos, S. A., S. C. A. Thomopolous, and C. N. Capsalis, "Genetic design of dual-band, switched-beam dipole arrays, with elements failure correction, retaining constant excitation coefficients," *J. of Electromagn. Waves and Appl.*, Vol. 20, No. 14, 1925–1942, 2007.
18. Rajarman, R., P. Gogineni, G. Prescott, and P. Kanagaratnam, "Design of a wideband vivladi antenna array for the snow radar," B.E. (Electronic & Communication Engg.), Coimbator Inst. of Tech., India 2001, February 2, 2004.